Journal of GeoEngineering, Vol. 19, No. 3, pp. 102-111, September 2024
http://dx.doi.org/10.6310/jog.202409_19(3).2

EFFECT OF SOIL NAILS INCLINATION ON STABILITY OF SOIL SLOPES

Kavya LR [1*], Aman Kumar [2], and Radhikesh Prasad Nanda [3]

ABSTRACT

This study aimed to use numerical modeling to investigate the behavior of soil slopes under various inclination angles of soil nails and surcharge load conditions. Numerical modeling and analysis are performed using finite element software PLAXIS 2D. In this study, the stability of a soil slope is investigated at different soil nail inclination angles, viz., 0°, 5°, 10°, 15°, 20°, 25°, and 30°. A surcharge load of 80 kN/m is applied at distances of 2 m, 4 m, and 6 m from the slope edge. The results show that the safety factor increases with increasing soil nail angle under a constant surcharge load. Similar results were obtained when the distance of the surcharge load increased from the slope edge. In addition, the bending moment and shear forces in the soil nails decreased with increasing inclination of the soil nails and increasing distance of the surcharge load from the slope edge. The slope with nails at 20° is the most stable slope, with safety factors of 1.647, 1.610, and 1.692 for the three surcharge loads. Similarly, minimum shear forces of 2.298, 2.684, and 1.183 kN/m and bending moments of 0.4132, 0.4075, and 0.1236 kN-m/m are predicted when the nails are inclined at 20° for the above three cases of surcharge loading, respectively.

Key words: Nailed soil slope, numerical modeling, finite element method, surcharge load, factor of safety.

1. INTRODUCTION

Sliding and instability on both natural and manmade slopes frequently occur anywhere in the world. The movement and sliding of soil or rock masses have disastrous impacts on communication lines, tunnels, water, sewage pipes, and structures. Sliding and instability harm or obstruct transport roadways, decrease their functionality and generally reduce their safety, which incurs high costs for inspection, maintenance, repair, and reconstruction on the part of the government. Soil nailing is an efficient method for improving the ground, particularly when there is slope instability. Soil nailing technology can be used to improve and stabilize unstable slopes. This involves inserting steel tendons into the soil to a specific depth and covering them with cement grout to stabilize the unstable soil walls caused by excavations and natural and manmade slopes. This approach has several benefits, including passive soil consolidation to prevent landslides, speed, ease of use, and low cost. It is necessary to examine the stability and strengthening techniques of these reinforced slopes.

Many studies have used the classic limit equilibrium approach to perform a stability analysis of reinforced slopes. The stability of soil slopes has been examined in numerous studies studies (Mandal and Mandal 2016; Biswas *et al.* 2017; Deng *et al.* 2017; Omid *et al*. 2020; Zewdu 2020). Greenwood (1990) changed the force balance approach when calculating slope safety factors by considering geosynthetic reinforcement. Patra and Basudhar (2005) presented an ideal computer-based design method for examining nailed-soil slopes. The ideal spacing, orientation, and diameter maximize the safety factor of the slopes as well as the critical slip surface. To satisfy the overall and internal equilibrium and consider the tensile resistance of the reinforcement, the authors employed a limit equilibrium formulation in this study. Fan and Luo (2008) and Garg *et al.* (2014) conducted experimental and numerical analyses to better understand the behavior of nailed soil slopes. They discovered that, in addition to slope geometry and soil characteristics, additional elements such as angle, length, spacing, and cable characteristics also significantly affect the stability of nailing slopes. Using the finite-element approach, Tan and Awam (2005) examined the effect of surcharges on the stability of nailing slopes. In Taman Pulai Emas, Johor Bahru, and Johor, on a permanent slope with a height of approximately 17 m in cohesionless soil, a case study was conducted to build a water tank for local use.

Concerns have been raised regarding the minimal safety factor when operating on a slope. Thus, slope nailing was proposed to increase safety. This study employed the SLOPE/W program to calculate the slope safety factor. This software is based on limit equilibrium. According to Wei and Cheng (2010), there are no appreciable differences between the limit equilibrium and strength reduction strategies regarding safety and slip surfaces. The distinction between the two approaches is apparent when the overburden stress regulates the nail load. Bushira *et al.* (2018) investigated a conceptual model of a real slope on the Wozeka-Gidole Road, which became unsuccessful. They compared the numerical outcomes of the SLOPE/W and PLAXIS programs using the finite-element method (FEM) and limit equilibrium approach. Sharma and Ramkrishnan (2020) carried out parametric optimization research utilizing the PLAXIS program based on finite element analysis as a numerical technique, considering the soil–nail interaction and back analysis of the nail pull-out strength. The findings demonstrated that the pull-out strength is a function of depth, allowing optimization of the nail length pattern. They then conducted a dynamic study to guarantee seismic stability by utilizing FHWA recommendations and numerical techniques such as FEM and LEM. Finally, they

Manuscript received April 27, 2024; revised May 26, 2024; accepted July 29, 2024.

[1*] Postgraduate Student, (corresponding author), Department of Civil Engineering, National Institute of Technology Durgapur, India. (e-mail: klr.21p10170@mtech.nitdgp.ac.in).

[2] Postgraduate Student, Department of Civil Engineering, National Institute of Technology Durgapur, India.

[3] Associate Professor, Department of Civil Engineering, National Institute of Technology Durgapur, India.

performed a numerical regression analysis to determine the association between geotechnical factors, nail length patterns, and limiting conditions to support the study and numerical studies. A seismic study of nailed soil slopes was conducted by Chavan *et al.* (2017), taking into account the impacts of the interface.

They created a 2D finite element model of a typical nailing slope while considering the nonlinearity and pressure dependence of the soil. The results show that the model of the nailing soil interface may significantly affect slope deformation. Additionally, the nail elastic modulus is useful only for steep slopes, but the nail tip plays a significant role in determining the failure mode and FOS of a nailed slope. They also discovered that the ideal placement of the soil nail is longer at the bottom and shorter at the top and that the slope status and failure mode impact the distribution of the tensile stress along the nail. Lin *et al.* (2013) used strength reduction and finite difference methods in FLAC3D software to investigate the impact of the nail length, direction, installation position, and horizontal distance on the FOS and slip surface of the slope on evaluating the nailed slope stability. Askari and Gholami (2017) conducted a numerical analysis of an ideal soil-nail configuration under various circumstances. They assessed the safety factor and displacement of the wall tip for a nailed wall using three geometries and two surcharge loads. Rawat and Gupta (2016) conducted a comparative study of nailed soil slopes using both the LEM and FEM methods. LEM analysis was performed using SLOPE/W software, whereas FEM analysis was performed using PLAXIS 2D software. The analysis was performed on a reference model reinforced by soil nails at angles of 0, 15, and 30°. The FEM and LEM methods showed that the soil slope had the highest stability between 15° and 30°. Kumar and Nanda (2024) performed a parametric study on effect of anchor angle on the stability of slope reinforced by pile-anchor structure under seismic load over a high cut slope. In this study they found that the slope is most stable when the anchor is inclined at 15° to the horizontal. Kaleshar *et al.* (2021) analyzed nailed soil slopes on a reference model using the finite difference method. The finite difference method was applied using FLAC 3D software. In this study, the behavior of nailed soil slopes under different surcharge load conditions was examined. As the distance of the surcharge load from the edge of the slope increased, the safety factor of the soil slope also increased.

The above studies show that soil nails provide better slope stability, which depends upon the nail angles and the surcharge load from the slope's edge. Considering the above two parameters, using the finite element method, a combined study is carried out with different nail angles and surcharge loads with varying positions from the edge of the slope.

2. NUMERICAL MODELING PROCEDURE

The finite element approach has gained widespread acceptance for the study of slope stability because it requires no assumptions regarding the location of the failure surface and interslice forces (Griffiths and Lane 1999). Analyses are becoming increasingly nonlinear and iterative owing to the growing utilization of complicated geometries and material data. Geometry and soil are functions of solutions in finite element formulations. It is advisable to utilize one of the FE packages because this process requires a large amount of calculation data and time. In the present investigation, PLAXIS 2D software is used to analyze the stability of soil slopes reinforced with soil nails at different angles under the influence of surcharge loads at different distances. This software uses FE analysis to split the continuum into discrete components and split each element into nodes. The degrees of freedom with discrete values for each node correspond to the unknowns in the problem with a given set of boundary conditions. The degrees of node freedom are connected to the displacement components in the current study. Each line element had three nodes, each of which had a different displacement value. These three nodes help to create six-node triangles, whereas a line element with five nodes creates a triangle with 15 nodes. In scenarios involving nails, anchors, or geogrids, 15-node triangles have been proven to produce more accurate results than six-node triangles (Brinkgreve *et al.* 2017). The link between the small incremental stress and strain also regulated the material in the FE analysis. The Mohr-Coulomb constitutive model is incorporated into the FEM software. This procedure replicates irreversible stress in a completely plastic environment.

A yield surface comprising a collection of yield functions is constructed to detect the presence of plastic points in the continuum. These yield functions are a result of the current stress and strain levels. The FEM procedure also makes it possible to mimic a material's elastic–perfectly plastic behavior. During the computations, the elastic and plastic fractions of these stresses and the strain rates were separated. According to Griffiths *et al.* (1982), the Mohr-Coulomb model has six yield functions of plastic soil factors, such as "c" and "ϕ". The stiffness of each component and, eventually, the total volume S & R of soil are determined by FE analysis using a material stiffness matrix that is created using these notions for material transition. The load advancement number of steps is used in the strength reduction method, which is also referred to as the ϕ-c reduction method. An incremental multiplier, M_{sf}, is used to reduce the strength parameters. The following equation is used to compute the safety factor:

$$SF = \frac{\text{available strength}}{\text{strength at failure}} = \text{value of } \sum M_{sf} \text{ at failure} \qquad (1)$$

The type of constitutive soil model chosen, type and size of the element, discretized mesh, node position for the displacement curve, and tolerance permitted for nonlinear analysis all affect the precision of the factor safety. The model is determined to have reached the final state, and depending on the FE method employed, either the maximum number of iterations is reached, the model experiences a continuous failure mechanism, or the chosen points in the continuum are subjected to a rapid shift in the displacement. For accurate model failure, FEM programs provide arc-length control, which is used throughout the iteration process. An abrupt failure of some points is occasionally observed during nonlinear analysis, which results in the formation of an "apparent" negative stiffness matrix beyond the final limit state. The arc-length control approach solves the snap-through issue in the FEM. The commercial finite element program PLAXIS now includes an arc-length control approach to provide dependable collapse loads for controlled-load computations. As a result, PLAXIS 2D, a robust and effective technique for determining the safety factor of slopes, is utilized in this study. It is based on the finite element method and includes an elastic, completely plastic (Mohr-Coulomb) stress–strain relationship.

The FE routine PLAXIS 2D v21.1 is used to numerically model the reinforced slopes. PLAXIS 2D uses a 15-noded triangulation procedure to account for the soil slope under plain strain. The dimensions, boundary conditions, and geotechnical properties are obtained from a study (Kaleshar *et al*. 2021) to simulate the model in the FEM, and a Mohr-Coulomb model with well-graded sandy

soil is utilized. The phreatic line was positioned at the base of the model considering the drained soil state. The PLAXIS program offers the option of employing geogrids, fixed-end anchors, node-to-node anchors, and plate elements as reinforcement systems. However, a plate element with an elastic equivalent can be utilized as a nail to strengthen slopes. The geometric models measured 28 m, 12 m, and 3 m in length, height, and breadth, respectively. The slope has an angle of 45°, and its edge is 16 m long. The Mohr-Coulomb constitutive model is the only one that appears reasonable and more acceptable than the others and can be employed with the given parameters because the material of the soil slope is cohesionless. The failure in this model is unaffected by the intermediate principal stress, which depends on the main and minor principal stresses. Consequently, the model is accepted and utilized for data analysis. This concept is typical for the plastic mode in soil and rock mechanics and suggests that materials are produced only under shear. Table 1 lists the physical and mechanical parameters of the soil-mass model (Kaleshar *et al.* 2021).

The nails are modeled as plate elements of a circular cross-section. Subsequently, the equivalent flexural rigidity and axial stiffness must be calculated for an accurate simulation of the soil nails. Babu and Singh (2009) provided a formula for obtaining the equivalent modulus of elasticity for simulated nails:

$$E_{eq} = E_n \frac{A_{nail}}{A} + E_g \frac{A_{grout}}{A} \tag{2}$$

Similarly, the equivalent axial stiffness is given by the relation

$$EA = \frac{E_n}{S_h} \frac{\pi}{4} d^2 \tag{3}$$

The relation gives the equivalent bending stiffness:

$$EA = \frac{E_n}{S_h} \frac{\pi}{64} d^4 \tag{4}$$

The equivalent plate diameter of the nail is calculated by the PLAXIS software using the following formula:

$$d_{eq} = \sqrt{12 \frac{EI}{EA}} \tag{5}$$

Equations (2)-(5) are used in the present study to calculate the nail input values used for the analysis, as shown in Table 2 (Rawat and Gupta 2016).

Table 1 Material properties of the soil layer

Density, ρ (kg/m^3)	1900
Young's modulus (Elastic modulus), E_s (MPa)	15
Poisson's ratio, ν	0.42
Internal friction angle, ϕ (°)	30
Cohesion, c (kPa)	5

Table 2 Physical and mechanical properties of the simulated nails

Nail element and nail type	Plate and elastic
Axial stiffness, EA (kN/m)	2.98×10^6
Flexural rigidity, EI (kN m^2/m)	113.64×10^3
Diameter of the nail, d_{eq}	12
Poisson's ratio, ν	0.35

The use of an interface with a virtual thickness factor (δ) of 0.1 ensures optimum soil-nail interactions. The element thickness is multiplied by the virtual thickness factor throughout the mesh generation process. The same material dataset allocated to the model is also provided to the interface. Without experimental data, an interface strength reduction factor (R_{inter}) of 1 was utilized to simulate the pull-out resistance of soil nails (Brinkgreve *et al.* 2017). The following relationship between the soil strength and the interface strength is established:

$$\frac{\tan\phi_{interface}}{\tan\phi_{soil}} = R_{inter} \quad \text{and} \quad \frac{c_{interface}}{c_{soil}} = R_{inter} \tag{6}$$

A total of 863 elements and 7127 nodes are generated in the meshing of the model when there is no reinforcement in the slope (Fig. 1).

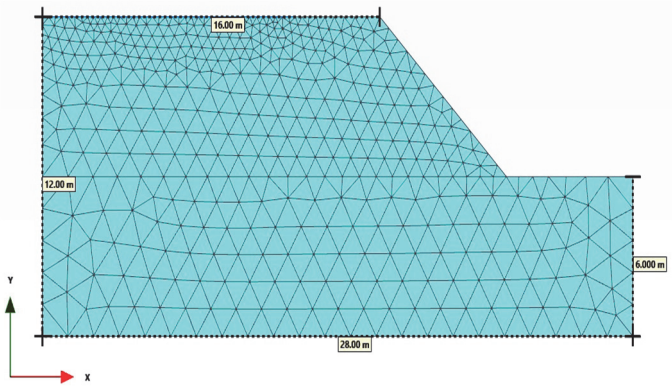

Fig. 1 The geometry and mesh of the model

2.1 Validation of the Model

The model presented in section 2 is validated with the models presented by Kaleshar *et al.* (2021) for the point load of 100 kN applied at a distance of 2, 3, 4, 6, and 8 m from the slope edge. Table 3 shows the factor of safety comparison between the proposed model and the model analyzed by previous investigator.

Table 3 clearly shows that the results obtained through the proposed model is in close argument with the result obtained by the previous researcher.

Table 3 Factor of safety comparison between the proposed model and the model proposed by Kaleshar *et al.* (2021)

Application of point load from slope edge	2 m	3 m	4 m	6 m	8 m
Kaleshar *et al.* (2021)	1.27	1.37	1.40	1.39	1.39
Proposed Model	1.27	1.37	1.40	1.41	1.42

3. NUMERICAL RESULTS AND ANALYSIS

3.1 Numerical Results

The soil slope is nailed at different angles with six nails 6 m in length and a horizontal spacing of 1 m. The different nailing systems used in this study are shown in Fig. 2.

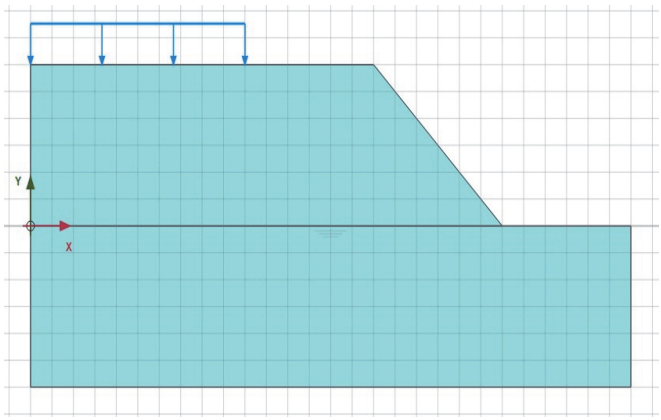

(a) No reinforcement

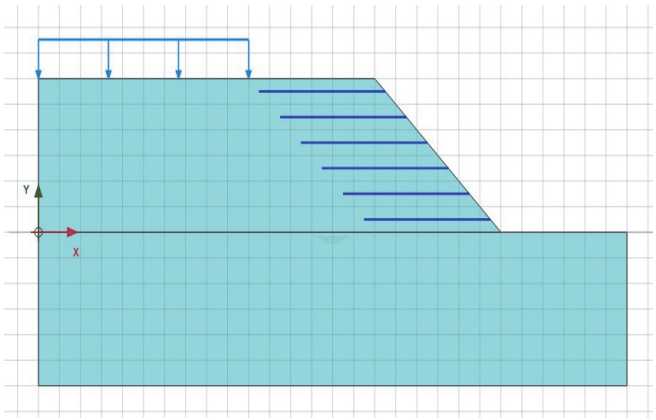

(b) Nails at 0°

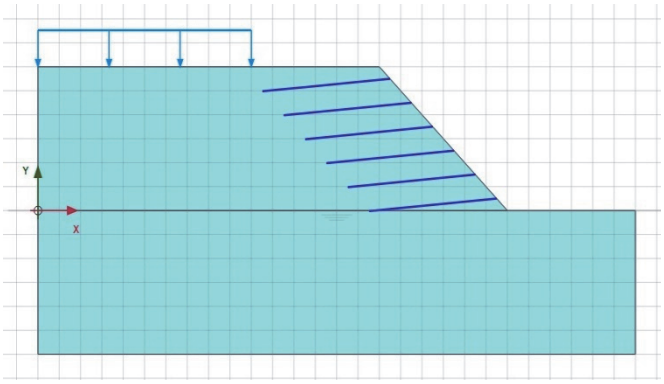

(c) Nails at 5°

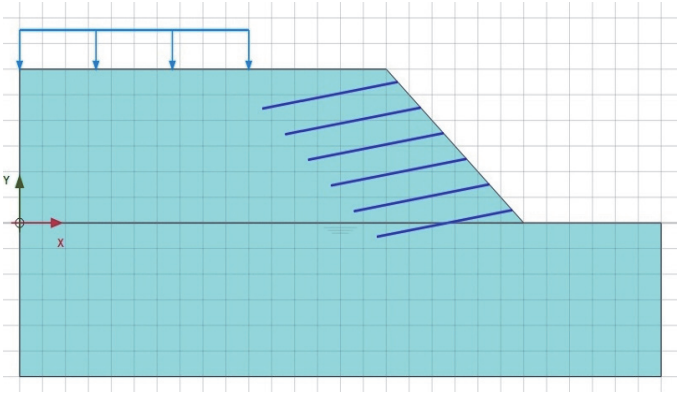

(d) Nails at 10°

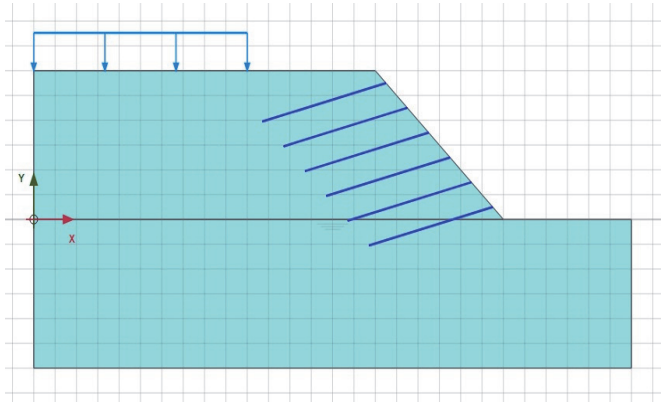

(e) Nails at 15°

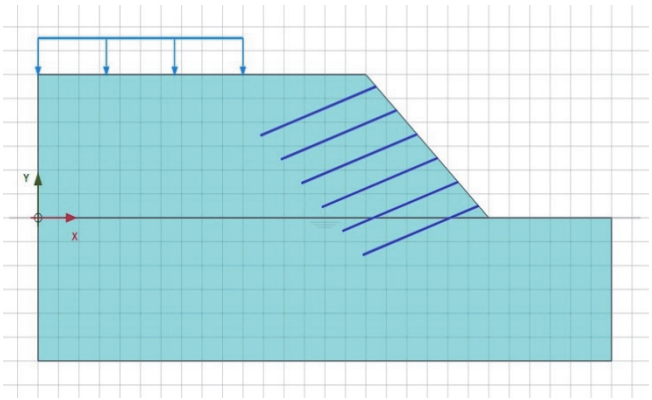

(f) Nails at 20°

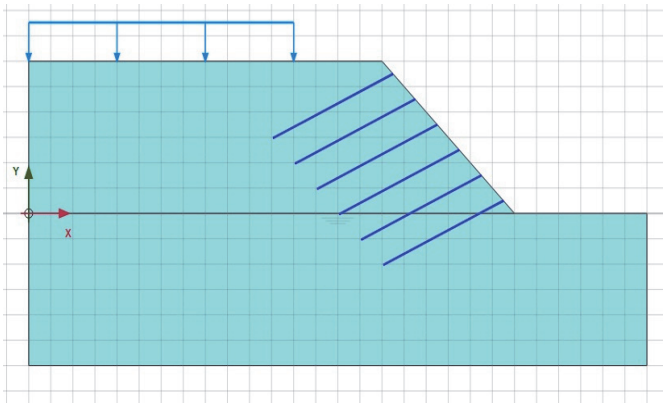

(g) Nails at 25°

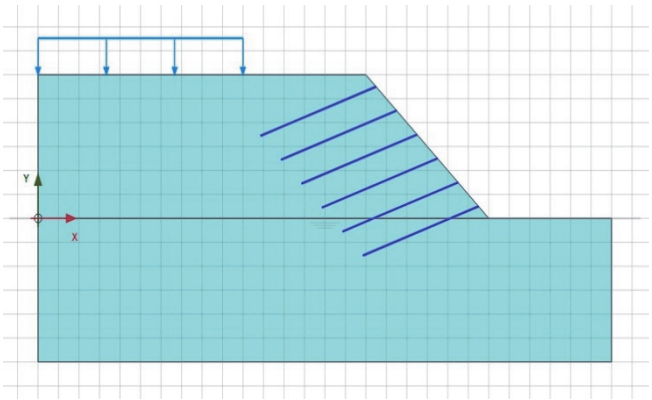

(h) Nails at 30°

Fig. 2 Different nailing conditions for the soil slope

Case 1: The surcharge load acts at a distance of 2 m from the slope edge

Table 4 lists the values of the safety factors for different reinforcement cases. The value of the safety factor increases for the soil slope as the angle of the soil nails increases. The surcharge load used in the analysis was 80 kN/m, acting vertically downward on the top surface of the slope.

The slip surface position can be estimated by examining the total deformations in the slope. The horizontal and vertical displacements of all the surcharge load types occurred in the negative x-direction.

Table 4 Factor of safety for different types of soil nails in slopes

Conditions	Factor of safety
Without soil nails	1.03
Slope reinforced with nails at 0°	1.31
Slope reinforced with nails at 5°	1.38
Slope reinforced with nails at 10°	1.49
Slope reinforced with nails at 15°	1.55
Slope reinforced with nails at 20°	1.65
Slope reinforced with nails at 25°	1.58
Slope reinforced with nails at 30°	1.40

The slip surface of a slope is the surface along which the slope is most likely to fail. It is generally considered the surface up to which the movement in the slope is different relative to the adjacent surface, and the movement is effective. The incremental deviatoric strain bands in the slope at different points under different conditions are shown in Fig. 3. The incremental deviatoric strain bands shows slip surfaces for different types of nails under different conditions. It is apparent that as the angle of the soil nails increases, the radius of the slip surface increases, which shows that there are fewer chances of failure of the slope system. The slip surface shows the maximum radius for a nail angle of 20°.

Case 2: The surcharge load acts at a distance of 4 m from the slope edge

As the distance of the surcharge load increases from the slope edge, changes in the deformations and factor of safety of the slope can be observed. This also affects the nailing system as the nail load increases.

In this case, the safety factor increases as the angle of the soil nail increases. However, when the safety factors were compared with those in Case 1, the safety factors in this case for each nailing condition decreased (Table 5).

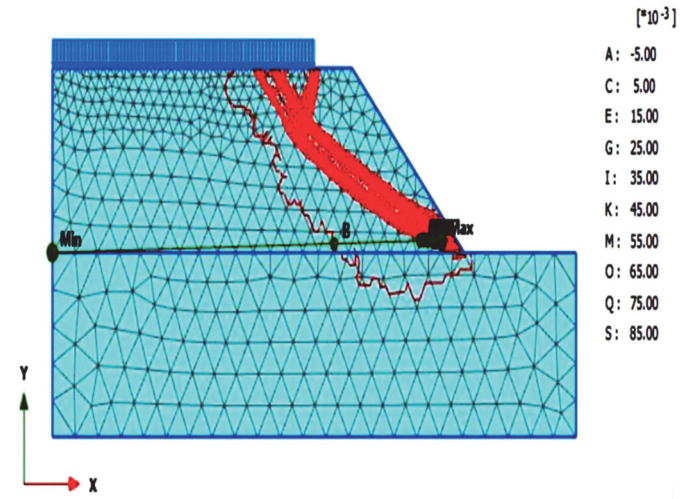

(a) Slip surface in no-nail case

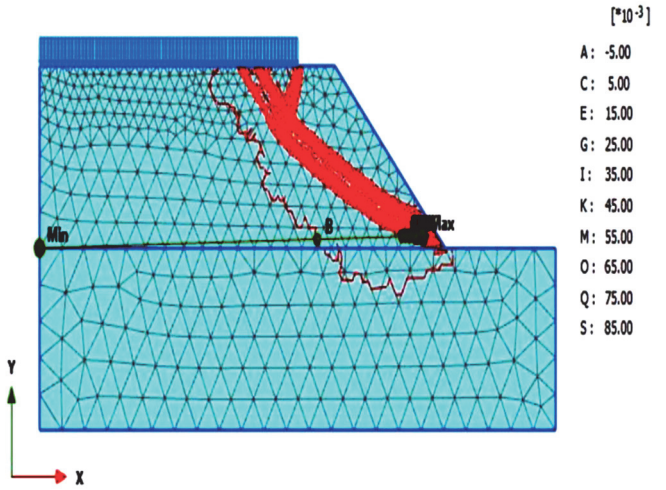

(b) Slip surface in the case of horizontal nails

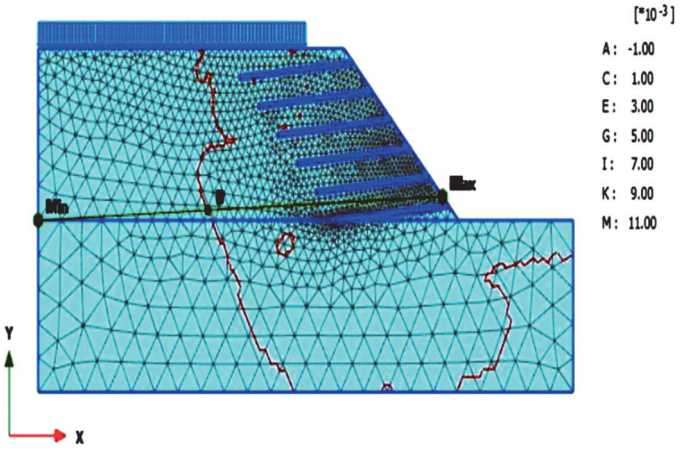

(c) Slip surface for nails at 5°

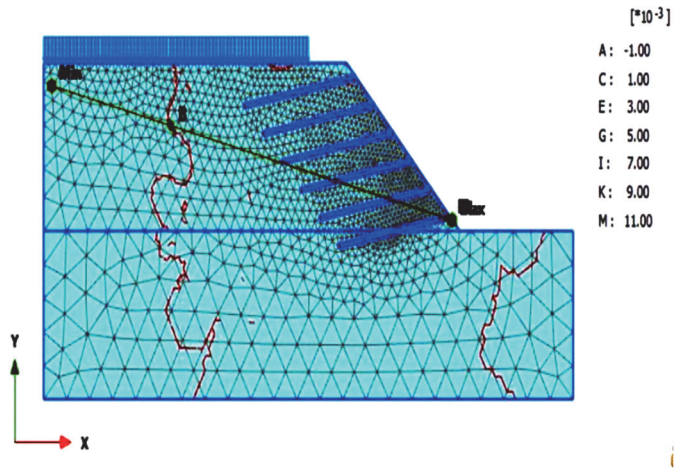

(d) Slip surface for nails at 10°

Fig. 3 Location of the slip surface for different nailings

In this case, the slip surfaces also exhibit behavior similar to that in Case 1. As the angle of the soil nails increased, the radius of the slip surface of the soil slope increased, ensuring a more stable slope. The shape of the deformed mesh of the slope model is shown in Fig. 4.

Table 5 Safety factors for different types of soil nails on slopes

Conditions	Factor of safety
Without soil nails	1.10
Slope reinforced with nails at 0°	1.31
Slope reinforced with nails at 5°	1.37
Slope reinforced with nails at 10°	1.48
Slope reinforced with nails at 15°	1.53
Slope reinforced with nails at 20°	1.61
Slope reinforced with nails at 25°	1.57
Slope reinforced with nails at 30°	1.44

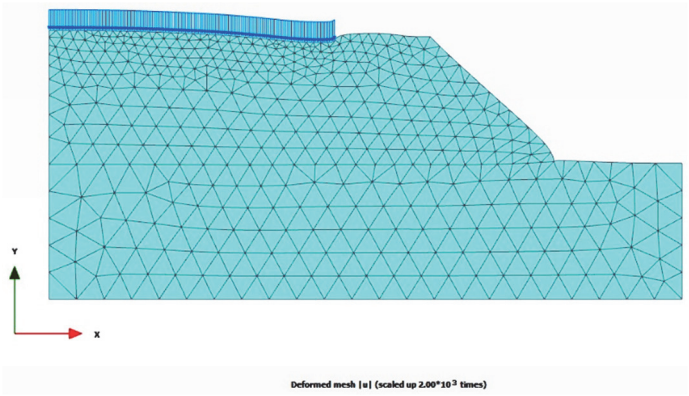

Fig. 4 Deformed mesh in the absence of soil nails

Case 3: The surcharge load acts at a distance of 6 m from the slope edge

In this case, a surcharge load of 80 kN/m is applied on the slope vertically downward, acting on the top of the slope at a distance of 6 m from the slope edge. The safety factors are very similar to those of Cases 1 and 2.

In this case, the slip surfaces exhibit similar behavior. They show an increase in the radius with an increase in the angle of the soil nails. From Table 6, it is evident that the safety factors increase with an increase in the angle of the soil nails up to 20°; after that, they start decreasing.

According to Tables 3, 4, and 5, the maximum safety factor was attained at an angle of 20° for the soil nails. The results of the different analyses also showed that the factor of safety increased the angle of the soil nails from 0° to 20°, but after 20°, the safety factors started decreasing gradually.

Table 6 Safety factors for different types of soil nails on slopes

Conditions	Factor of safety
Without soil nails	1.11
Slope reinforced with nails at 0°	1.45
Slope reinforced with nails at 5°	1.51
Slope reinforced with nails at 10°	1.58
Slope reinforced with nails at 15°	1.62
Slope reinforced with nails at 20°	1.69
Slope reinforced with nails at 25°	1.43
Slope reinforced with nails at 30°	1.41

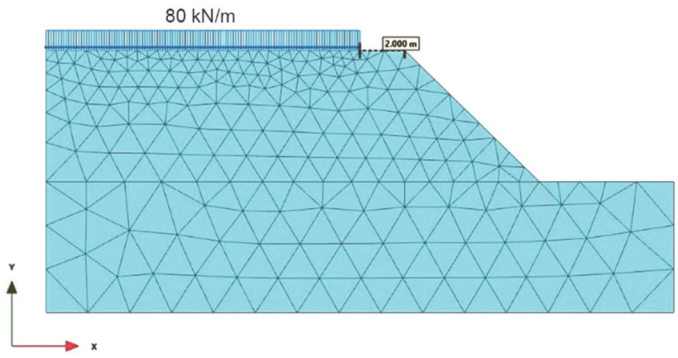

(a) Loading conditions in Case 1

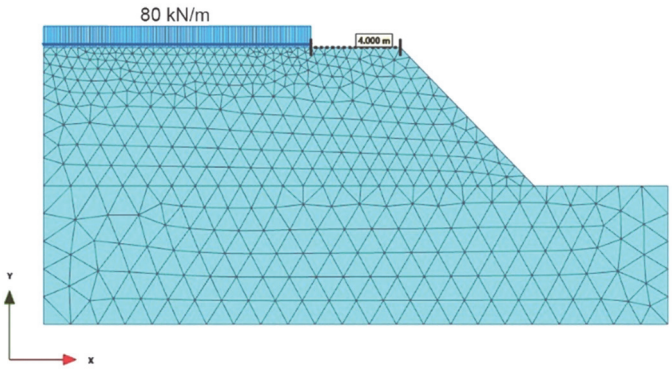

(b) Loading conditions for Case 2

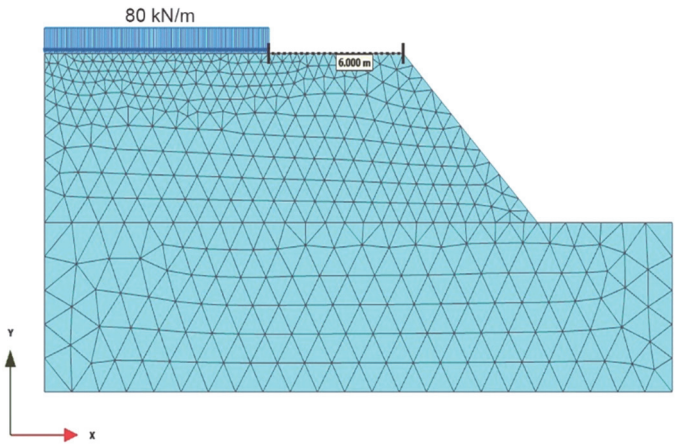

(c) Loading conditions for Case 3

Fig. 5 Surcharge load at the soil slope in different cases

3.2 Internal Forces of Soil Nails

The internal forces include the shear force and bending moment generated in the nails by the application of surcharge loads. In this study, the shear force generated in the nails decreased with increasing inclination angle of the soil nails. Under the loading conditions of Case 1 (Fig. 5(a)), the maximum shear forces are 9.59 kN/m and 2.30 kN/m, which are generated in soil nails inclined at 0° and 20°, respectively. Table 7 shows the different values of the shear force generated at different inclinations of the soil nails. Similarly, under the loading conditions of Case 2 (Fig. 5(b)) and Case 3 (Fig. 5(c)), the maximum and minimum shear forces were generated at 0° and 20°, respectively. The shear forces generated in Cases 2 and 3 are listed in Tables 8 and 9, respectively.

Table 7 Shear force in Case 1

Nail angle (°)	Maximum shear force (kN/m)	Percentage reduction (%)
0	9.59	
5	4.51	53.00
10	4.24	55.96
15	3.71	61.37
20	2.30	76.04
25	3.21	66.57
30	5.88	38.66

The maximum reduction in shear force compared to the shear force of nails inclined at zero degrees is shown by the nails inclined at 20°, which is equal to 76.04%.

Table 8 clearly shows that the maximum value of the shear force generated in the soil nail is 8.82 kN/m at an inclination of 0°, and the minimum shear force is 2.68 kN/m in the nail inclined at 20°. The percentage reduction was greatest in the nail inclined at 20° (69.58%).

In Case 3, a maximum reduction of 85.05% is observed in the shear forces of the nails. The shear forces in the soil nails in all three cases showed that as the distance of the surcharge load from the edge of the soil slope increased, the shear force generated in the soil nails decreased (Table 9).

The bending moment in Case 1 (Fig. 5(a)) is maximal when the slope is reinforced horizontally with nails and minimal when the nails are inclined at an angle of 20°. Table 10 lists the different bending moments generated in the soil nails in Case 1.

Table 8 Shear force in Case 2

Nail angle (°)	Maximum shear force (kN/m)	Percentage reduction (%)
0	8.82	
5	7.73	12.35
10	5.09	42.34
15	2.87	67.45
20	2.68	69.58
25	3.99	54.79
30	4.65	47.26

Table 9 Shear force in Case 3

Nail angle (°)	Maximum shear force (kN/m)	Percentage reduction (%)
0	7.91	
5	3.81	51.85
10	3.21	59.37
15	1.71	78.44
20	1.18	85.05
25	2.75	65.30
30	4.77	39.76

Table 10 Bending moment in Case 1

Nail Angle (°)	Maximum bending moment (kN-m/m)	Percentage reduction (%)
0	1.09	
5	0.86	21.19
10	0.83	23.41
15	0.72	33.77
20	0.41	62.06
25	0.68	37.21
30	0.87	20.11

From Table 10, it is observed that the maximum reduction in the bending moment is shown when the soil nails are inclined at 20° compared with horizontal soil nails. The maximum value of the bending moment is 1.09 kN/m at the horizontal nails, and the minimum value of the soil nails is 0.41 when the nails are at an inclination of 20°. Similar types of behavior are shown by the nails in Case 2 and Case 3; the maximum bending moment is generated when the nails are horizontal, and a minimum bending moment is generated when the nails are at an inclination of 20°.

From Tables 11 and 12, it is evident that the bending moment decreases with increasing inclination angle of the soil nails. In all the cases, the bending moment reached a maximum when the nails were horizontal and a minimum when the nails had an inclination of 20°.

From Fig. 6, it is evident that the reduction in shear forces increases with an increase in the inclination of the soil nails. It can also be concluded that the maximum reduction in shear force occurs in Case 3, and the maximum variation in the reduction in shear force occurs in Case 2. However, at 20°, the shear force increased gradually in all the cases.

From Fig. 7. It can be concluded that the bending moment decreases with an increase in the angle of inclination of the soil nails, but it increases after a 20° inclination. The maximum bending moment is observed in Case 2 when the end of the line load

Table 11 Bending moment in Case 2

Nail angle (°)	Maximum bending moment (kN-m/m)	Percentage reduction (%)
0	1.42	
5	1.05	26.41
10	0.67	51.54
15	0.54	61.72
20	0.41	71.30
25	0.63	55.93
30	0.85	40.41

Table 12 Bending moment in Case 3

Nail angle (°)	Maximum bending moment (kN-m/m)	Percentage reduction (%)
0	0.92	
5	0.89	3.37
10	0.45	51.35
15	0.36	61.31
20	0.12	86.63
25	0.29	68.58
30	0.46	50.63

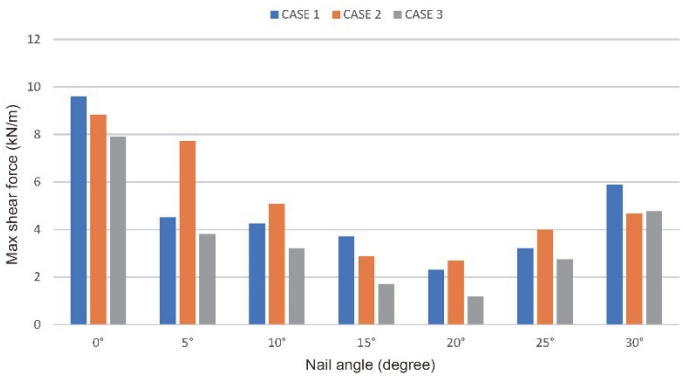

Fig. 6 Shear force in soil nails in different cases

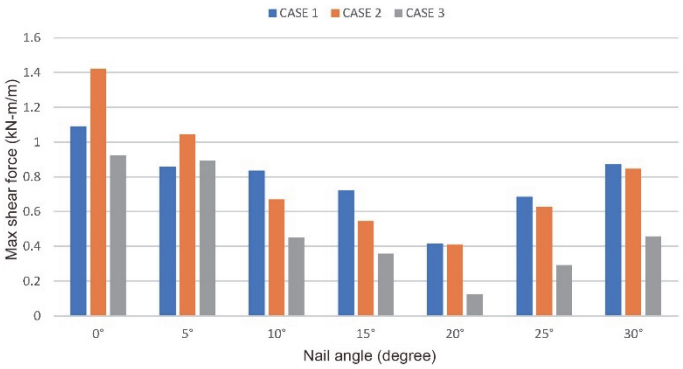

Fig. 7 Bending moment in soil nails in different cases

is almost in the middle of the soil nails. It can also be concluded that the distance of the surcharge line load from the slope-edge bending moment and shear force tends to decrease.

The maximum axial force in the nails continued to increase as the inclination angle of the soil nails increased. A similar variation in nail axial force was discovered by Shiu and Chang (2006), who observed that it increased up to a nail inclination of 20° in the horizontal direction before decreasing to zero at a nail inclination of 65°.

The factor of safety and internal forces obtained in different cases show that 20° is the best angle for reinforcing soil slopes with soil nails (Fig. 8). Figure 8 also shows that the axial force in the soil nails decreases as the distance of the surcharge load from the edge of the slope increases.

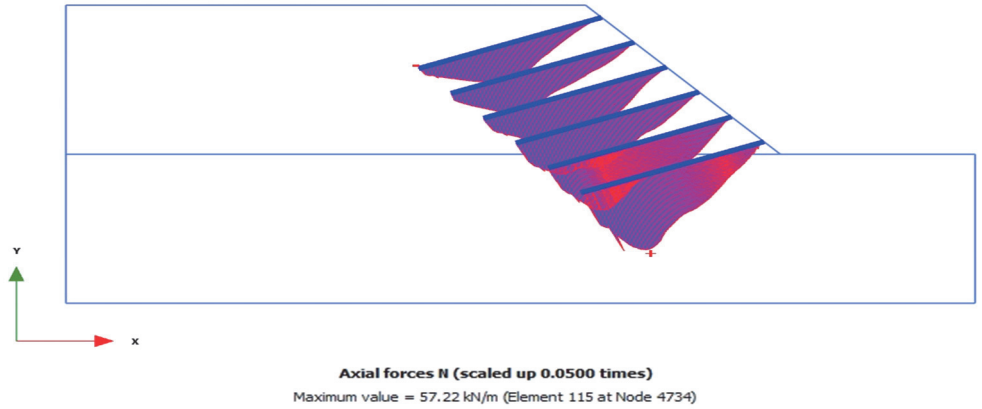

(a) Axial force in Case 1

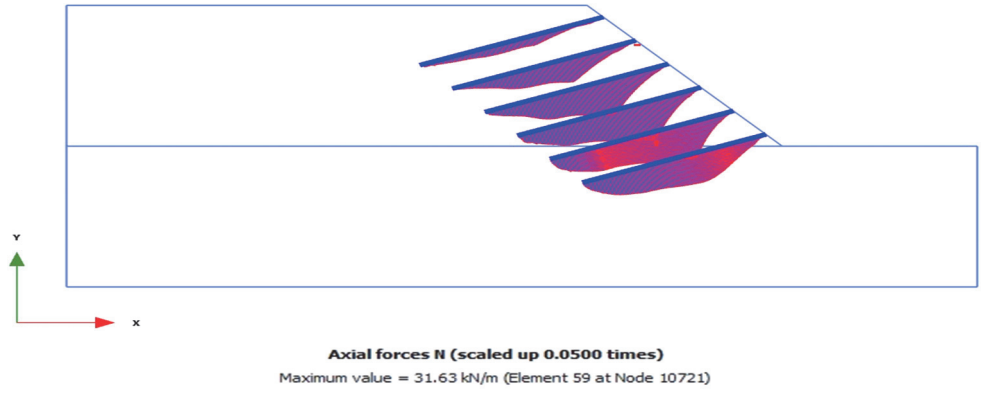

(b) Axial force in Case 2

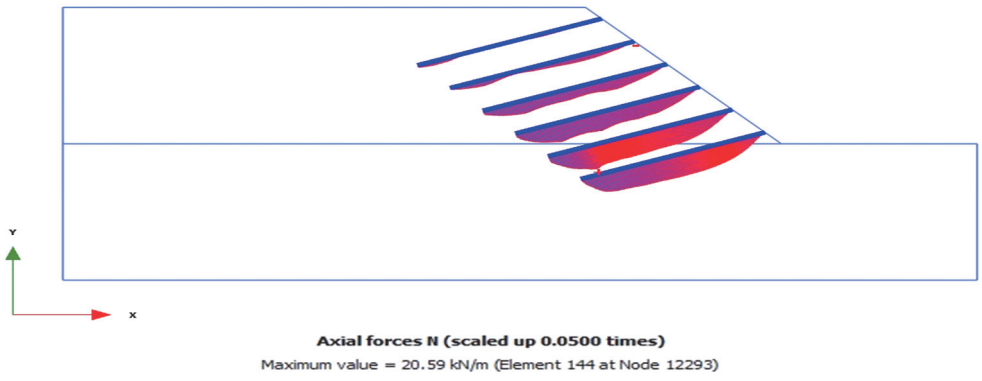

(c) Axial force in Case 3

Fig. 8 Axial force in different cases when nails are inclined at 20°

3.3 The Interface Effect of Soil Nail and Surrounding Soil

The soil nail and surrounding soil interface may affect the slope stability response. The interaction between the soil nail and the surrounding soil is simulated by applying interface elements. In PLAXIS, R_{inter} values are used to define the interface elements. R_{inter} values are known as the shear strength reduction factor. Analysis with R_{inter} values from 0.6 to 1 have been conducted in the lack of data regarding interface strength. Slopes reinforced by nails at 20° inclination from all three loading cases are taken for the analysis. Figure 9 shows that as we increase the value of R_{inter} from 0.6 to 1, the value of the factor of safety also increases. Additionally, it showed that the bending stiffness and axial stiffness values included in the finite element analysis change for FOS, slip surfaces, deformed mesh, and nail forces.

Figure 10 shows that the bending moment decreases with increased R_{inter} values. This indicates that as we increase the shear strength reduction factor, the shear strength of the soil surrounding the nail is getting mobilized, resulting in a decrease in the bending moment generated in the soil nail.

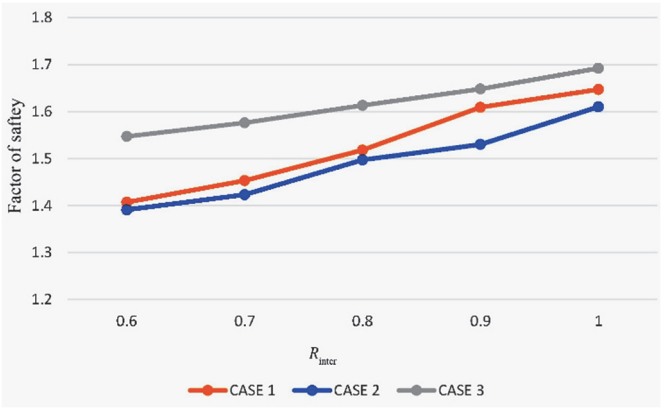

Fig. 9 Variation of factor of safety with R_{inter}

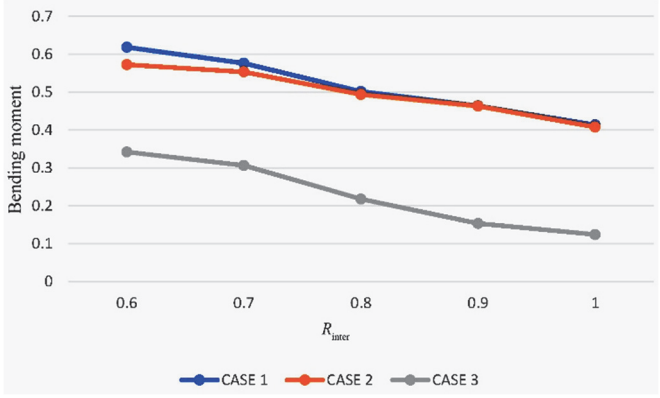

Fig. 10 Variation of bending moment with R_{inter}

4. CONCLUSIONS

In this study, the effect of soil nail inclination on the stability of soil slopes is analyzed considering a surcharge load of 80 kN/m at a different position from the slope edge. From the study, the following conclusions are drawn:

1. The slip surface radius increases with increasing soil nail inclination, ensuring a more stable slope. With an increase in the angle of the soil nails, the slip surface lines approach the toe because of the increase in the slip radius, which increases the slope stability.
2. For unreinforced slopes, the factor of safety increases as the distance of the surcharge from the edge of the slope increases; however, for nailed slopes, the factor of safety is minimal when the surcharge load is near the slope edge.
3. The most stable slope is reinforced with soil nails at an angle of 20° for the surcharge load at different positions. The factor of safety is found to be 1.65, 1.61, and 1.69 when the distance of the surcharge load from the slope edge is 2 m, 4 m, and 6 m, respectively.
4. The maximum shear force decreased as the angle of inclination of the soil nails increased. The percentage decrease in shear force compared with that of horizontal nails and nails inclined at 20° was 76.04%, 69.58%, and 85.05% when the distance of the surcharge load from the slope edge was 2 m, 4 m, and 6 m, respectively.
5. The shear force generated in the soil nails decreases as the distance of the surcharge load from the edge of the slope increases. For the 20° soil nail inclinations, the shear force is found to be 2.30, 2.68, and 1.18 kN/m for the above three surcharge loadings, respectively.
6. A similar response is predicted for the bending moment. The maximum bending moment in the soil nails also decreases with increasing inclination angle. The percentage decrease in the bending moment of the soil nails inclined at 20° was estimated to be 62.05%, 71.03%, and 86.62% when the distance of the surcharge load from the slope edge was 2 m, 4 m, and 6 m, respectively.
7. It is also predicted that the bending moment generated in the soil nails decreases as the distance of the surcharge load from the edge of the slope increases for a particular soil nail angle. For 20° nails, the bending moments are found to be 0.41, 0.40, and 0.12 kN/m for the above three surcharge locations.
8. It is observed that the interface parameter, *i.e.,* shear strength reduction factor, between soil nail and surrounding soil affects the slope stability response. With the increase in the value of the shear strength reduction factor, the safety factor of the slope increases while the bending moment generated in the soil nail decreases.

The present study focused on the stability of soil slopes using soil nails at different angles with different surcharge loads at three different distances from the slope edge. This study considers a constant soil slope (45°) with a fixed soil nail strength and length. However, the sensitivity of the other terrain conditions (slope angle) may affect the soil nail response. Hence, further analysis of different terrain conditions and soil nail lengths may be considered in future studies. Further surcharge loads may behave differently during earthquake excitation. Therefore, such a study can be extended to other dynamic loads.

FUNDING

The authors received no funding for this work.

DATA AVAILABILITY

The data and/or computer codes used/generated in this study are available from the corresponding author on reasonable request.

CONFLICT OF INTEREST STATEMENT

The authors declare that there is no conflict of interest.

REFERENCES

Askari, A. and Gholami, A. (2017). "Effect of nail's orientation and length on soil-nailed retaining structures' stability." *DFI Journal - The Journal of the Deep Foundations Institute*, **11**(1), 30-38. https://doi.org/10.1080/19375247.2017.1416569

Babu, G.L.S. and Singh V.P. (2009). *Simulation of Soil Nail Structures using PLAXIS 2D*. PLAXIS Bulletin 16-21.

Biswas, R.N. and Islam, M.N. (2017). "Modeling on management strategies of slope stability and susceptibility to landslides catastrophe at hilly region in Bangladesh." *Modeling Earth Systems and Environment*, **3**(3), 977-998. https://doi.org/10.1007/s40808-017-0346-4

Brinkgreve, R., Engin, E., and Swolfs, W. (2017). *Plaxis 2D Manual*. Rotterdam, Netherlands, Balkema.

Bushira, K.M., Gebregiorgis, Y.B., Verma, R.K., and Sheng, Z. (2018). "Cut soil slope stability analysis along National Highway at Wozeka–Gidole Road, Ethiopia." *Modeling Earth Systems and Environment*, **4**(2), 591-600. https://doi.org/10.1007/s40808-018-0465-6

Chavan, D., Mondal, G., and Prashant, A. (2017). "Seismic analysis of nailed soil slope considering interface effects." *Soil Dynamics and Earthquake Engineering*, **100**, 480-491. https://doi.org/10.1016/j.soildyn.2017.06.024

Deng, G., Xu, T., Chen, R., Lu, Z., and Liu, J. (2018). "Numerical analysis on stabilizing mechanism of soil nails in steep fill slopes subjected to rainfall infiltration using a hypoplastic model." *Arabian Journal for Science and Engineering*, **43**(10), 5079-5090. https://doi.org/10.1007/s13369-017-2937-9

Fan, C.C. and Luo, J.H. (2008). "Numerical study on the optimum layout of soil–nailed slopes." *Computers and Geotechnics*, **35**(4), 585-599. https://doi.org/10.1016/j.compgeo.2007.09.002

Garg, A., Garg, A., Tai, K., and Sreedeep, S. (2014). "An integrated SRM-multi-gene genetic programming approach for prediction of factor of safety of 3-D soil nailed slopes." *Engineering Applications of Artificial Intelligence*, **30**, 30-40. https://doi.org/10.1016/j.engappai.2013.12.011

Greenwood, J.H. and Jewell, R.A. (1990). "Strength and safety: the use of mechanical property data." *Reinforced Embankments. Theory and Practice. Proceedings of the Conference Reinforced Embankments,* September 27 1989.

Griffiths, D., Smith, I.M., and Molenkamp, F. (1982). "Computer implementation of a double-hardening model for sand." in *Proc. IUTAM Conf. on Deformation and Failure of Granular Materials*. Delft, Netherlands 213-221.

Griffiths, D.V. and Lane, P.A. (1999). "Slope stability analysis by finite elements." *Géotechnique*, **49**(3), 387-403. https://doi.org/10.1680/geot.1999.49.3.387

Kalehsar, I.R., Khodaei, M., Dehghan, A.N., and Najafi, N. (2022). "Numerical modeling of effect of surcharge load on the stability of nailed soil slopes." *Modeling Earth Systems and Environment*, **8**(1), 499-510. https://doi.org/10.1007/s40808-021-01087-7

Kumar, A. and Nanda, R.P. (2024). "Effect of anchor angle on the stability of slope reinforced by pile-anchor structure under seismic load." *Indian Geotechnical Journal*. https://doi.org/10.1007/s40098-024-00936-3

Lin. H., Xiong, W., and Cao, P. (2013). "Stability of soil nailed slope using strength reduction method." *European Journal of Environmental and Civil Engineering*, **17**(9), 872-885. https://doi.org/10.1080/19648189.2013.828658

Mandal, B. and Mandal, S. (2016). "Assessment of mountain slope instability in the Lish River basin of Eastern Darjeeling Himalaya using frequency ratio model (FRM)." *Modeling Earth Systems and Environment*, **2**(3), 121-121. https://doi.org/10.1007/s40808-016-0169-8

Omid, N., Ali, N.D., and Kaveh, A. (2020). "Evaluation of geometrical parameters affecting on the optimal slope design of Shadan Gold-Copper Open Pit Mine." *Journal of Mining Engineering*, **15**, 28-44. https://doi.org/10.22034/ijme.2020.114926.1754

Patra, C.R. and Basudhar, P.K. (2005). "Optimum design of nailed soil slopes." *Geotechnical and Geological Engineering*, **23**(3), 273-296. https://doi.org/10.1007/s10706-004-2146-7

Rawat, S. and Gupta, A.K. (2016). "Analysis of a nailed soil slope using limit equilibrium and finite element methods." *International Journal of Geosynthetics and Ground Engineering*, **2**(4), 34-34. https://doi.org/10.1007/s40891-016-0076-0

Sharma, A. and Ramkrishnan, R. (2020). "Parametric optimization and multi-regression analysis for soil nailing using numerical approaches." *Geotechnical and Geological Engineering*, **38**(4), 3505-3523. https://doi.org/10.1007/s10706-020-01230-8

Shiu, Y. and Chang, G. (2006). *Effects of Inclination Length Pattern and Bending Stiffness of Soil Nails on Behaviour of Nailed Structures*. Geotechnical Engineering Office, Civil Engineering and Development Dept, Hong Kong (China). OCLC Number 243532470

Tan, C.C. and Awam, F.K. (2005). *Application of Soil Nailing as Protection and Reinforcement for Slope Stabilization*. Universiti Teknologi Malaysia. [e-book]

Wei, W.B. and Cheng, Y.M. (2010). "Soil nailed slope by strength reduction and limit equilibrium methods." *Computers and Geotechnics*, **37**(5), 602-618. https://doi.org/10.1016/j.compgeo.2010.03.008

Zewdu, A. (2020). "Modeling the slope of embankment dam during static and dynamic stability analysis: a case study of Koga dam, Ethiopia." *Modeling Earth Systems and Environment*, **6**(4), 1963-1979. https://doi.org/10.1007/s40808-020-00832-8